A Novel Rotation-Mitigation Technology for Cycling Helmets Tested Across Helmet Types, Impact Locations and Headforms

Domna-Maria Kaimaki[a,*], Higor Alves de Freitas[a], Archie G. D. Read[a], Theodore D. M. Dickson[a], Tony White[a], Henry C. A. W. Neilson[b]

Head rotation is the leading cause of diffuse brain injuries from cycling accidents, with severe, long-term or even fatal consequences. Here, we present a novel helmet safety technology, the Release Layer System (RLS), designed to enhance conventional helmets and reduce the likelihood of such injuries. RLS is located on the outer side of the helmet and thus, gets impacted first. The force of the impact activates a rolling mechanism triggering the release of an outer polycarbonate panel, thereby dispersing and transforming a substantial portion of the incident rotational energy. To evaluate the effectiveness of the technology, we conducted oblique impact tests on three popular helmet types, each in conventional and RLS-equipped configurations, tested on three impact locations and using two headforms. RLS-equipped helmets reduced Peak Angular Velocity (PAV) by 57-66%, averaged across impact locations, compared to their conventional counterparts. This corresponds to a 68-86% reduction in the probability of an AIS2+ brain injury, as estimated by the Brain Injury Criterion. The most notable improvement was observed at the pYrot location (frontal, on-axis impacts), with up to 85% PAV reduction. Testing across headforms further demonstrated the effectiveness of the technology in mitigating head rotation irrespective of variations in evaluation setups. This work introduces a novel mechanism for rotational impact mitigation and provides evidence of its potential benefits compared with conventional helmets. As an outer-layer approach, RLS may offer an alternative pathway for managing rotational kinematics in future helmet designs.

Keywords: Head Protection, Oblique Impact, Rotation-Mitigation Helmet Technology, RLS, Traumatic Brain Injury Prevention, Vulnerable Road Users

1 Introduction

Within the last decade, cycling has experienced a notable rise in popularity with the global number of bicycles estimated to be over a billion[1,2]. As cycling activity increases, so too does the number of associated incidents. In Europe, cyclists are the only mode of transport that has shown almost no decline in fatalities over the past decade, while also making up 24% of all serious injuries in 2020[3]. In response, a multidisciplinary body of research has emerged to better understand and mitigate risks within an increasingly complex and dynamic road environment. The interaction between Vulnerable Road Users (VRUs) and motorised vehicles has been further investigated using video data for accident reconstructions[4,5], while comprehensive databases - integrating police reports, clinical records, and insurance claims - have been developed to support injury analysis[6,7]. At the same time, advances in sensor technology and computer vision methods are being used to suggest infrastructure updates and explore real-time accident prevention strategies[8], and policy recommendations are increasingly being drawn from case studies such as the Netherlands, Denmark and Germany[9–11].

While systemic changes to infrastructure and policy are crucial, interventions at the individual cyclist level offer more immediate and actionable safety benefits. Cyclist head injuries are consistently identified as the most prevalent and severe risk, making helmets the primary focus of cyclist protective equipment[12–14]. Over the years, conventional helmets have undergone various material and design improvements so as to effectively reduce the transmission of impact forces to the head and, in doing so, lower the risk of Traumatic Brain Injury (TBI)[15,16]. This protective ability of helmets is assessed via standardised linear impact tests, as defined by certification protocols (EN 1078 for Europe, CPSC 1203 for the US, AS/NZS 2063 for Australia and New Zealand, and JIS T 8134 for Japan[17–20] as examples). However, such testing only replicates focal head injuries, such as skull fractures, neglecting head rotation and its effect to brain injury, which has long been established[21]. Advances in research connecting medical imaging and clinical outcomes to brain modelling and biomechanics, has shown that head rotation is responsible for concussions, certain types of haematomas, and diffuse axonal injuries (DAIs). While such pathologies may arise from mild Traumatic Brain Injuries (mTBIs), they have been linked to long-lasting impairments in sleep quality, motor function, memory, as well as more severe neurological damage and even death[22].

As a result, efforts to adapt helmet certification standards to reflect real-world oblique impacts, inducing both linear and rotational head kinematics, are currently underway. However, while a lengthy regulatory transition period is ongoing, helmet manufacturers have addressed this issue by introducing various technologies designed to complement the linear impact protection of conventional helmets by mitigating rotational energy transfer[23]. It is within this context that we introduce the Release Layer System (RLS) technology for cycling helmets.

1.1 State of the art & the Release Layer System (RLS)

Conventional helmets typically consist of at least two material layers: (i) an outer shell - commonly a thermoformed sheet of polycarbonate - that sustains the impact, distributes forces over a

[a]HEXR Ltd, 7 Corsican Square, London, E3 3YD, United Kingdom. [b]Dropmatics Ltd, 3 Hylands Yard, Rye, TN31 7EP, United Kingdom. E-mail: maria@hexr.com

larger area, and absorbs energy through deformation or fracture, and (ii) a liner, often made of expanded polystyrene (EPS) that absorbs and dissipates energy through compression, providing cushioning to minimise head injuries. Over the past two decades, conventional helmets have been supplemented with additional materials aimed at mitigating the rotational energy transmitted to the head during an impact to address the leading cause of mTBIs. Technologies such as MIPS, SPIN, WaveCel, Koroyd, KinetiCore and Rheon have been integrated into the interior of helmets presenting a meaningful advancement in the helmet's effectiveness in mitigating rotation[24–29].

Here, we present a different approach to rotation mitigation: an outer technology, called the Release Layer System (RLS). The RLS technology consists of an array of polycarbonate spheres of 2.0 ± 0.1 mm in diameter, attached onto a flexible membrane and encapsulated between an outer polycarbonate shell, such as that found in a conventional EPS helmet ('B-surface'), and an additional polycarbonate shell ('A-surface') split into panels. The polycarbonate spheres are held in place by adhesives on the top and bottom, while the assembly of membrane and spheres is secured onto a helmet by a combination of bonding with the B-surface using an adhesive, and mechanical interlocking with the A-surface using fasteners (Figure 1A). During an impact, the oblique force on the A-surface panel severs the mechanical fasteners and the adhesive connections of the spheres in the impacted area allowing the spheres to roll freely, while the panel releases from the B-surface. This mechanism operates on a principle analogous to that of ball bearings, enabling relative rotational motion between outer helmet layers through a rolling interface. The rolling of the spheres disperses and transforms a substantial portion of the energy of the impact, thereby protecting the head from rotational acceleration (Figure 1B), and is complemented by the EPS liner, which absorbs part of the remaining energy through compression[30].

RLS can be integrated into a variety of helmets; in this work it has been implemented in urban, road and mountain-bike (MTB) helmets (helmet types making up 83% of all helmets rated by Virginia Tech Helmet Ratings[31]). In urban helmets, RLS appears as a single membrane with spheres between surfaces A and B. In road and MTB helmets, RLS is split into multiple parts of the same composition, to accommodate helmet features, such as vents, that are crucial for helmet comfort. This is also mirrored in the A-surface, which is split into multiple panels. In this publication, we present helmets with one, three and four panels for urban, road and MTB helmets, respectively (Figure 1C), and experimentally assess the effectiveness of the RLS technology in mitigating head rotation by performing oblique impact testing of conventional and RLS-equipped cycling helmets of all three types.

2 Materials & methods

2.1 Helmets

All helmets were manufactured by HEXR Ltd (London, UK) or its partners. The conventional helmets comprised of EPS (nominal density of 70 g/l) and a polycarbonate shell, similarly to the majority of cycling helmets on the market. The polycarbonate shell was formed to have cavities that could be used for the addition of the RLS technology. The RLS-equipped helmets had the same composition and geometry as the conventional helmets with the addition of the RLS technology and the A-Surface on the outer side (Figure 1A,C, Table S1 in Supplementary Information).

2.2 Headforms & instrumentation

The majority of the experiments in this publication were conducted with the 50th percentile male Hybrid III headform (58 cm head circumference, Humanetics Innovative Solutions Inc, Michigan, United States) that has been widely used for the evaluation of helmets[25,26,32]. These experiments were conducted at the iCUBE laboratory of the University of Strasbourg (UNISTRA) with a HIII headform equipped with a triaxial linear accelerometer (PCB Piezotronics, New York, United States) and angular rate sensors (ATA Sensors, New Mexico, United States) measuring in the SAE J211 orientation. The accelerometers are located at the center of gravity of the headform and have an amplitude range of ± 500 g and a sampling rate of 25.6 kHz by channel, while the angular rate sensors have a measurement capacity of ± 8000 deg/s, a bandwidth of 1 kHz and a sampling rate of 25.6 kHz.

Further testing with a second, newly developed, headform was also conducted. The EN 17950 headform was used (57 cm head circumference, Humanetics Innovative Solutions Inc, Michigan, United States) which was developed under the instruction of the European Committee for Standardization Working Group 11 (CEN/TC158/WG11), with the aim to be a more biofidelic model of a human head, both in terms of its moments of inertia (MoIs) and its coefficient of friction (CoF), addressing criticisms faced by the other available headforms[33–35]. This testing was conducted at the HEXR laboratory due to the limited availability of the headform, compatible instrumentation, and related equipment (eg. COF measurement setup) in other laboratories at the time of the study. Prior to testing, the headform was cleaned following instructions by the manufacturer and its CoF was quantified against a structured polyester strap complying with EN 12195-2, as specified in the BS EN 17950:2024 standard[36]. The CoF was measured before and after testing (all tests were completed in one day) and the mean of each test sequence was found to be within the acceptable range (0.30 ± 0.03 N/m, Table S2 in Supplementary Information); during testing the headform was handled with gloves to minimise contamination. The EN 17950 headform is equiped with 6DX Pro-A instrumentation (DTS, California, United States), located at the headform's center of gravity, including a triaxial accelerometer (amplitude range of ± 500 g and bandwidth of 5kHz) and angular rate sensor (amplitude range of ± 8000 deg/s and bandwidth of 2kHz).

2.3 Impact testing methodology

Oblique impact testing was conducted using a drop tower (AD Engineering at UNISTRA and custom-made at the HEXR laboratory) comprising of a trolley to hold the helmet-headform assembly, stainless steel rails to guide the trolley with the testing assembly to the appropriate height, and a $45 \pm 0.5°$ stainless steel anvil (diameter of 130 ± 3 mm). The anvil surface was covered with

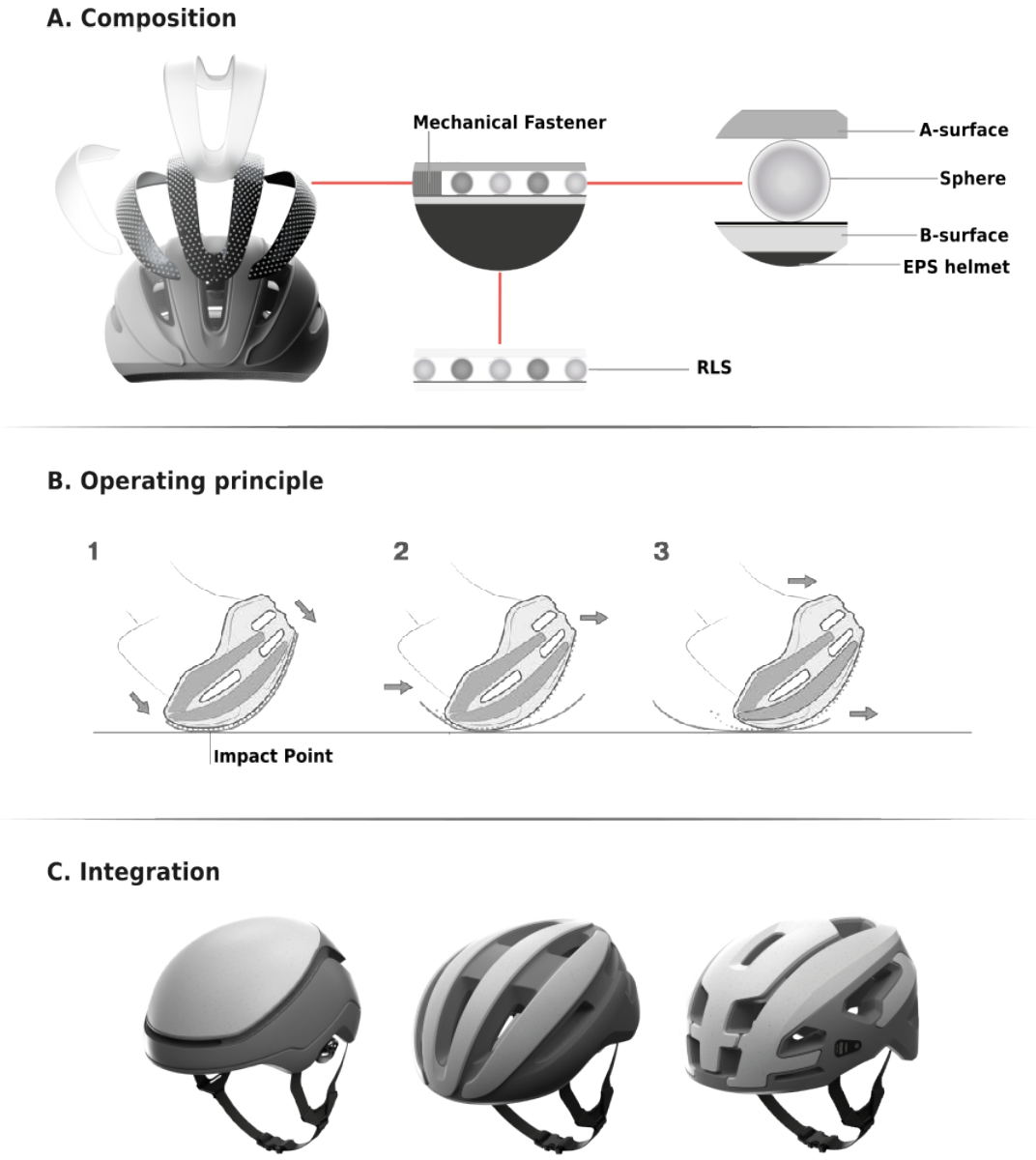

Fig. 1 The Release Layer System (RLS) in cycling helmets. A. A deconstructed RLS-equipped helmet, presenting the composition of the technology, B. The operating principle of the RLS technology during an impact, C. The integration of the RLS technology onto the different helmet types tested in this study; the urban, road and mountain bike helmets are displayed from left to right.

P80 abrasive paper, which was replaced after significant damage was observed. In order to assess the variability of the results, we conducted 4 repeats at each of the 3 impact locations (pXrot, pYrot and pZrot) for each helmet type (urban, road, MTB) and configuration (conventional and RLS-equipped). This resulted in $n = 72$ impacts with the Hybrid III headform at UNISTRA. Testing at the HEXR laboratory was conducted with the same number of repeats but using only the urban helmet resulting in $n = 24$ impacts with the EN 17950 headform (Table S1 in Supplementary Information). All tests were performed on undamaged helmets to assess their effectiveness against a single critical event. MTB helmets were tested without visors[29,37].

Prior to testing, the helmets were stored at a room temperature of $20 \pm 2°$C and a relative humidity of $50 \pm 20\%$ for a period of at least 4 hours; conditions that were maintained throughout the duration of the experiments. The headform was first aligned with the helmet using a nose gauge (indicating a normal distance of 63 mm between the tip of the nose and the helmet brim, Figure 2A). The impact speed for all testing was set to 6.5 m/s and tests were conducted on three impact locations chosen to represent real-life conditions based on the reconstruction of 1024 bicycle accidents[38]. The headform-helmet system was positioned in the drop tower according to the impact location required for testing. For pXrot and pYrot impacts, the central vertical axis of the headform (z-axis) was aligned to the vertical with a tolerance of $\pm 1°$, while the assembly (xy-plane) was placed at $0 \pm 1°$ around the z-axis from the front. The normal vector of the impact surface was parallel to the yz-plane and xy-plane, for pXrot and pYrot, respectively with a tolerance of $\pm 1°$. For pZrot impacts, the assembly was inclined by $65 \pm 1°$ around the y-axis from the base of the headform with the horizontal plane (the yz-plane was placed at $25 \pm 1°$ from the horizontal, Figure 2B). Inclinometers (High Precision Digital Level TLL-90S, Jingyan Instruments, China) were used in both laboratories to ensure alignment. This methodology follows closely the oblique testing protocol implemented by Folksam with an increase of the impact speed to $6.5\ \mathrm{m/s} \pm 0.1\ \mathrm{m/s}$ to align with the higher impact speed suggested in the provisional EN 1078:2025 standard[32].

2.4 Data acquisition and analysis

Once alignment was ensured, the headform-helmet assembly was secured in place to ensure its position does not vary as the trolley is raised (using tape at UNISTRA and a pneumatic actuator at HEXR). Subsequently, the instrumentation was armed and the trolley was raised to the required height as determined by a speed-height calibration protocol. The trolley was then released initiating a free fall of the assembly and the impact was recorded (Figure 2C). The actual impact velocity was measured using a light gate (BeeSpi V Light Gate, Vitta Education, United Kingdom). Additionally, a high speed video (Chronos 2.1 HD High Speed Camera, Kron Technologies, Canada) was recorded to visualise the impact and to further assess the alignment of the headform-helmet assembly on the drop tower post-impact. An AD Engineering data acquisition system and Sliceware were used at UNISTRA and the HEXR laboratory, respectively to collect and preprocess the kinematic data. The raw data from both laboratories was filtered with a CFC 1000 for linear acceleration and a CFC 180 for angular velocity, in accordance with ISO 6487[39].

The results are primarily presented in terms of peak values of key kinematic metrics: peak linear acceleration (PLA), peak angular velocity (PAV) and peak angular acceleration (PAA), where the angular acceleration is calculated by numerical differentiation from the angular velocity data (first-order finite difference). To quantify the variability of these metrics, descriptive statistics such as standard deviation and coefficient of variation (CV) were calculated. The effectiveness of the RLS technology is quantified as the percentage reduction in such metrics in comparison to conventional helmets ($\Delta_{RLS} = \frac{conventional - RLS}{conventional} \times 100\%$). Inferential comparisons between RLS-equipped and conventional helmets were conducted using statistical tests selected based on the underlying data characteristics. Specifically, the Shapiro-Wilk test and Levene's test were used to assess the assumptions of normality and homoscedasticity, respectively. Based on the outcome of these assumption tests, either Welch's ANOVA (for normally distributed data with unequal variances) or the Mann-Whitney U test (for non-normally distributed data) was applied as appropriate. All statistical analysis was conducted using custom Python code (v3.10.13) including the following libraries: pandas, numpy, scipy, matplotlib, statsmodels and pingouin. Beyond the evaluation of peak kinematics, the data was also used to estimate the risk of mild Traumatic Brain Injury (mTBI) and assess the potential of the RLS technology to mitigate such injuries. For this purpose, we employed the Brain Injury Criterion (BrIC) incorporating direction-specific thresholds for critical angular velocities. These thresholds were based on values derived from the cumulative strain damage measure (CSDM), maximum principal strain (MPS), and their average, as reported by Takhounts et al[40]. The resulting BrIC values were used to estimate the probability of sustained Abbreviated Injury Scale 2 or higher (AIS2+) injuries (Equations 1 and 2 in Supplementary Information).

3 Results

3.1 Average RLS effectiveness for three helmet types

The effectiveness of the conventional helmets was examined first as they will be used to establish the baseline throughout this study. The average PLA across all conventional helmets was 116-127g, which is approximately half of the PLA threshold included in the EN 1078:2012 standard (250 g)[17]. The average PAV across conventional helmets was 33-34 rad/s, while the average PAA was 6.7-7.3 krad/s^2. On the other hand, the average PLA across all RLS-equipped helmets was 109-116g (Δ_{RLS} of 4.5-9.7%). This reduction is not significant for urban and MTB helmets ($U = 97.0$, $p = 0.157$ and $U = 92.0$, $p = 0.260$, respectively), but it is significant for road helmets ($U = 129.0$, $p = 0.001$). In terms of rotational kinematics, the average PAV across all RLS-equipped helmets was 11-15 rad/s (Δ_{RLS} of 57-66%), while the average PAA was 2.9-4.1 krad/s^2 (Δ_{RLS} of 44-56%). Examining the data further (Table 1), the highest reduction in average rotational kinematics in comparison to conventional helmets is seen in the road helmet type (Δ_{RLS} of 66% in PAV and 56% in PAA), followed by the MTB

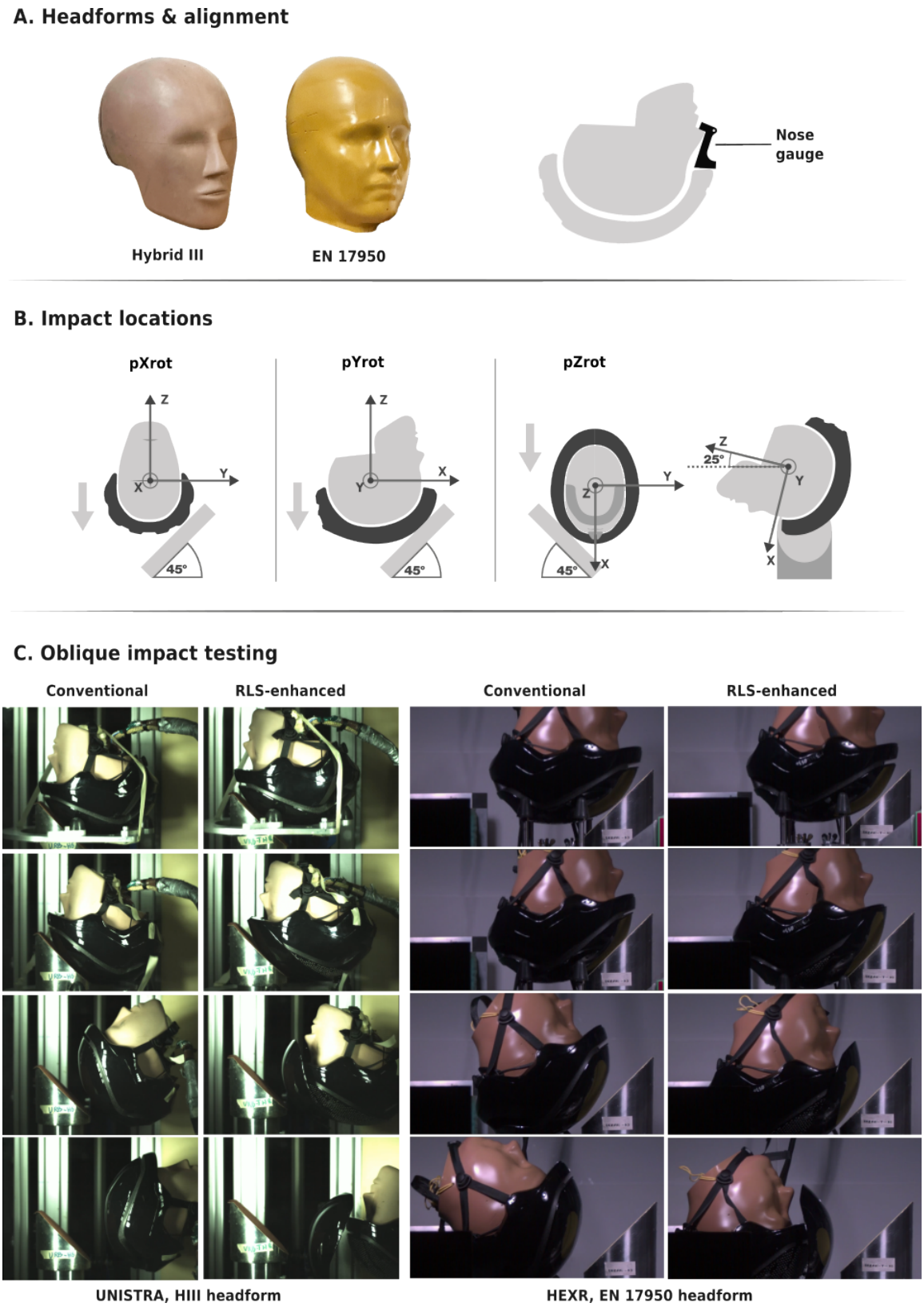

Fig. 2 The testing methodology of this study. A. The two headforms (Hybrid III & EN17950) that were used for impact testing and the nose gauge of 63 mm that was used for alignment of the helmet-headform assembly. B. The alignment of the headform-helmet assembly on the anvil for each impact location (pXrot, pYrot and pZrot) used for oblique testing. C. Snapshots of the high speed videos during oblique impact testing at UNISTRA and our laboratory for visual comparison of rotation on conventional and RLS-equipped helmets.

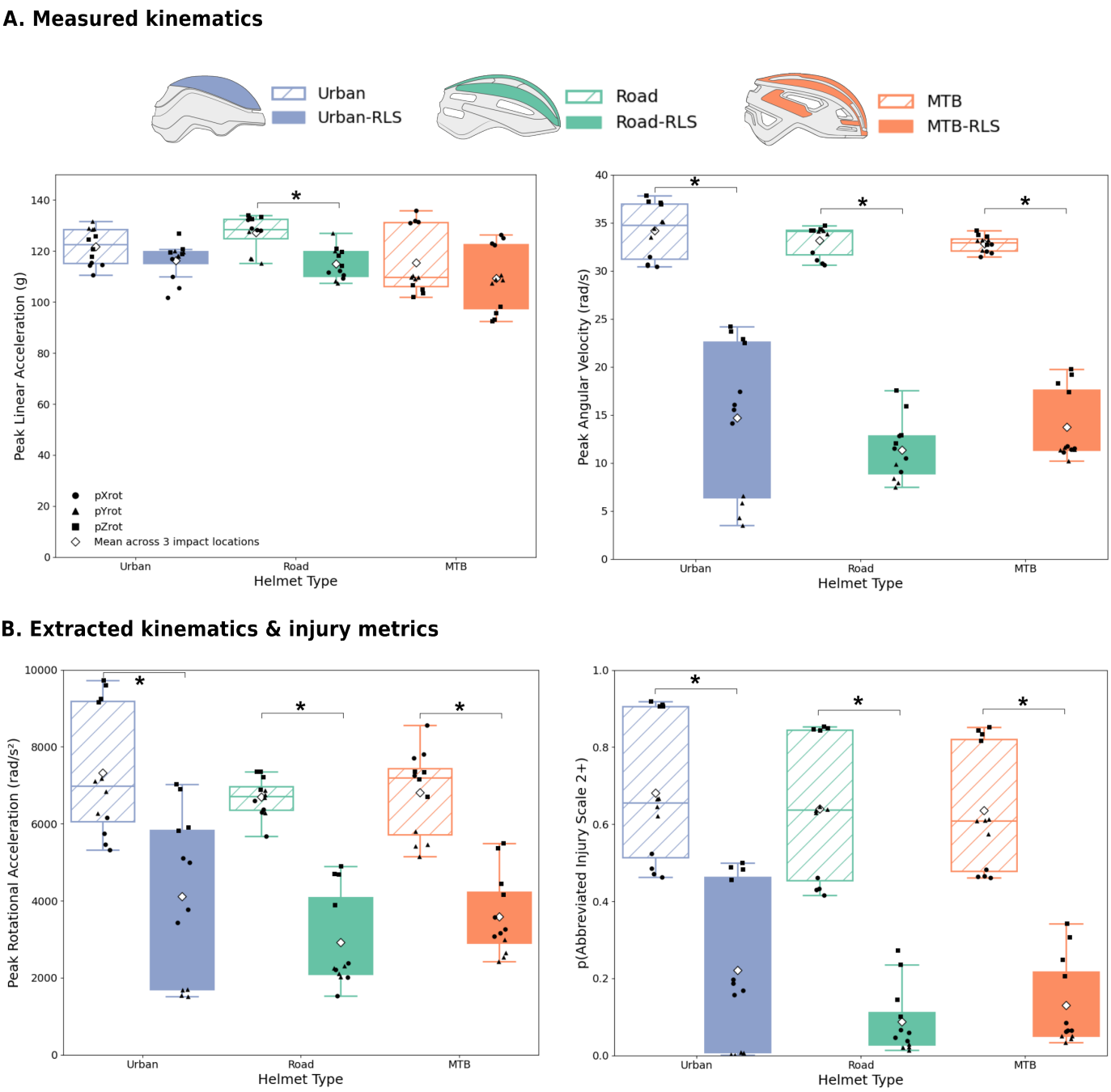

Fig. 3 Data for conventional (hatched) and RLS-equipped helmets (solid) by helmet type (indicated by color) averaged across three tested impact locations. Peak kinematics (PLA, PAV) as measured by the sensors are shown in A and calculated peak kinematics and injury metrics (PAA, AIS2+) are shown in B, with * indicating $p < 0.05$.

helmet type (Δ_{RLS} of 58% in PAV and 47% in PAA) and finally the urban helmet type (Δ_{RLS} of 57% in PAV and 44% in PAA). This trend can also be visualised in Figure 3, where the empty diamonds show the mean across all three impact locations for each helmet type and statistical differences are indicated with an asterisk. The decrease in rotational kinematics presented by RLS-equipped helmets of all three helmet types can then be translated into a reduction in the average risk of an AIS2+ injury across impact locations (Δ_{RLS} of 68-86%). In simple terms, this data suggests that a cyclist wearing the conventional urban, road or MTB helmets tested in this study is 68%, 64% or 64% likely to suffer a mTBI of AIS2+, such as a concussion or even loss of consciousness of up to 1 hour, if involved in an accident[41]. The probability of a similar injury being sustained if the cyclist wears the equivalent RLS-equipped helmet is significantly reduced to 22%, 9% and 13% for the urban, road, or MTB helmet, respectively.

However, assessing the effectiveness of the RLS technology by solely considering the average values is not sufficient. As illustrated in Figure 3, the results vary with impact location (black circles, triangles and squares representing pXrot, pYrot and pZrot

Table 1 Mean and standard deviation averaged across three locations (n=12 repeats) of the PLA, PAV, PAA, BrIC and probability of AIS 2+ for three helmet types. All PAV, PAA, BrIC and p(AIS2+) comparisons between conventional and RLS-equipped helmets were statistically significant with $U = 126.0 - 144.0$ and $p \leq 0.002$. Comparisons in PLA show a difference depending on helmet type and thus, the Mann-Whitney U test results are included in the table.

	Urban		Road		MTB	
Metric	Conventional	RLS	Conventional	RLS	Conventional	RLS
PLA (g)	121.8 ±7.2	116.3±7.1	127.3±7.0	115.0±6.2	115.5±12.9	109.3±12.7
	$U = 97.0$, $p = 0.157$		**U = 129.0, p=0.001**		$U = 92.0$, $p = 0.260$	
PAV (rad/s)	34.2±2.8	14.7±7.9	33.2±1.6	11.3±3.1	32.8 ±0.8	13.7±3.7
PAA (krad/s^2)	7.32 ±1.67	4.12 ±2.12	6.69 ±0.49	2.92 ±1.24	6.81 ±1.10	3.60 ±1.05
BrIC	0.65 ±0.13	0.32 ±0.18	0.62 ±0.11	0.24 ±0.09	0.61 ±0.12	0.28 ±0.09
p(AIS2+)	0.68 ±0.18	0.22 ±0.21	0.64 ±0.18	0.09 ±0.09	0.64 ±0.16	0.13 ±0.11

results, respectively). The urban helmet shows the highest variability in all rotational kinematics and injury metrics between locations, while the road and MTB helmets have a narrower spread. The implications of this variability for Δ_{RLS} are explored in the following section.

3.2 RLS effectiveness by impact location for three helmet types

The data collected for conventional and RLS-equipped helmets was examined per impact location with pXrot and pYrot simulating on-axis side and frontal impacts, respectively, while pZrot simulating off-axis frontal impacts. All comparisons of rotational kinematics and extracted injury metrics were statistically significant, irrespective of the helmet type ($U = 16.0$, $p = 0.029$ in Table 2 and indicated by the asterisk in Figure 4.) The largest Δ_{RLS} in PAV was observed at the pYrot location (85%, 75% and 66% for the urban, road and MTB helmets, respectively), followed by the pXrot location (49%, 65% and 64% for the urban, road and MTB helmets, respectively) and finally the pZrot location (38%, 57% and 44% for the urban, road and MTB helmets, respectively).

PYrot was also the most effective location for the RLS technology in terms of the probability of an AIS2+ injury, as calculated by the BrIC. Specifically, when wearing an RLS-equipped helmet, the probability of sustaining an AIS2+ injury is 1-4%, corresponding to a Δ_{RLS} of 93-98%. It is worth noting that while in the least effective location, pZot, the equivalent probability of an AIS2+ injury is increased to 19-48%, that still corresponds to a Δ_{RLS} of 47-78%.

3.3 RLS effectiveness across headforms

The Hybrid III headform was used for the bulk of the testing presented in this publication for direct comparison with the majority of the literature on cycling helmets[23,32]. In order to assess the robustness of the technology's effectiveness in mitigating rotational kinematics, we conducted additional testing with the urban helmets using a second headform, the EN 17950. We then compared the benefit offered by the technology, Δ_{RLS}, when tested with each of the two headforms (Table 3, Figure 5).

For the PLA, a statistical difference in Δ_{RLS} was shown in the pYrot location. This is more indicative of the fact that when testing with the EN 17950, the conventional and RLS-equipped helmets show no significant difference in pYrot PLA, while they do when they are tested with Hybrid III (Figure S2 in Supplementary Information). The potential influence of the technology on linear kinematics is further examined in the Discussion, with reference to the data from 3.2. For the rotational kinematics (PAV and PAA), no statistical difference in Δ_{RLS} was found in any of the impact locations, suggesting that the RLS-effectiveness in mitigating rotation is headform-agnostic. Despite that, statistical differences in injury metrics were found across most locations. While the direction of these differences is mostly favourable for the RLS technology (Δ_{RLS} in pAIS2+ is shown to increase for both the pXrot and the pZrot locations to 71.4% from 63.3% and to 64.6% from 47.1%, respectively, when using the EN 17950), more in-depth analysis is needed to better understand the underlying reasons for this variation.

4 Discussion

This study evaluated the effectiveness of cycling helmets equipped with the Release Layer System (RLS) compared with conventional EPS helmets, with a focus on rotational kinematics and the associated risk of mTBI. Across three helmet types and multiple impact locations, RLS integration substantially reduced rotational metrics and the corresponding injury risk, while producing smaller and less consistent improvements in linear kinematics. The following discussion expands on these findings by examining their broader implications, contributing factors, and areas for further investigation.

4.1 Evaluation of conventional helmets

The conventional helmets of all three helmet types tested exhibited PLA values well within the limits of the EN 1078:2012 standard[17], and their PAV and PAA values were consistent with those reported in previous studies of commercial helmets[25–27], suggesting that they are a representative baseline. The rotational performance of the conventional helmets corresponded to an average AIS2+ injury probability of 64-68% across all impact locations, indicating a high risk of mTBI in the event of an accident and the need for improved protection. Integration of the RLS technology substantially reduced rotational kinematics (Δ_{RLS} of 57-66% in

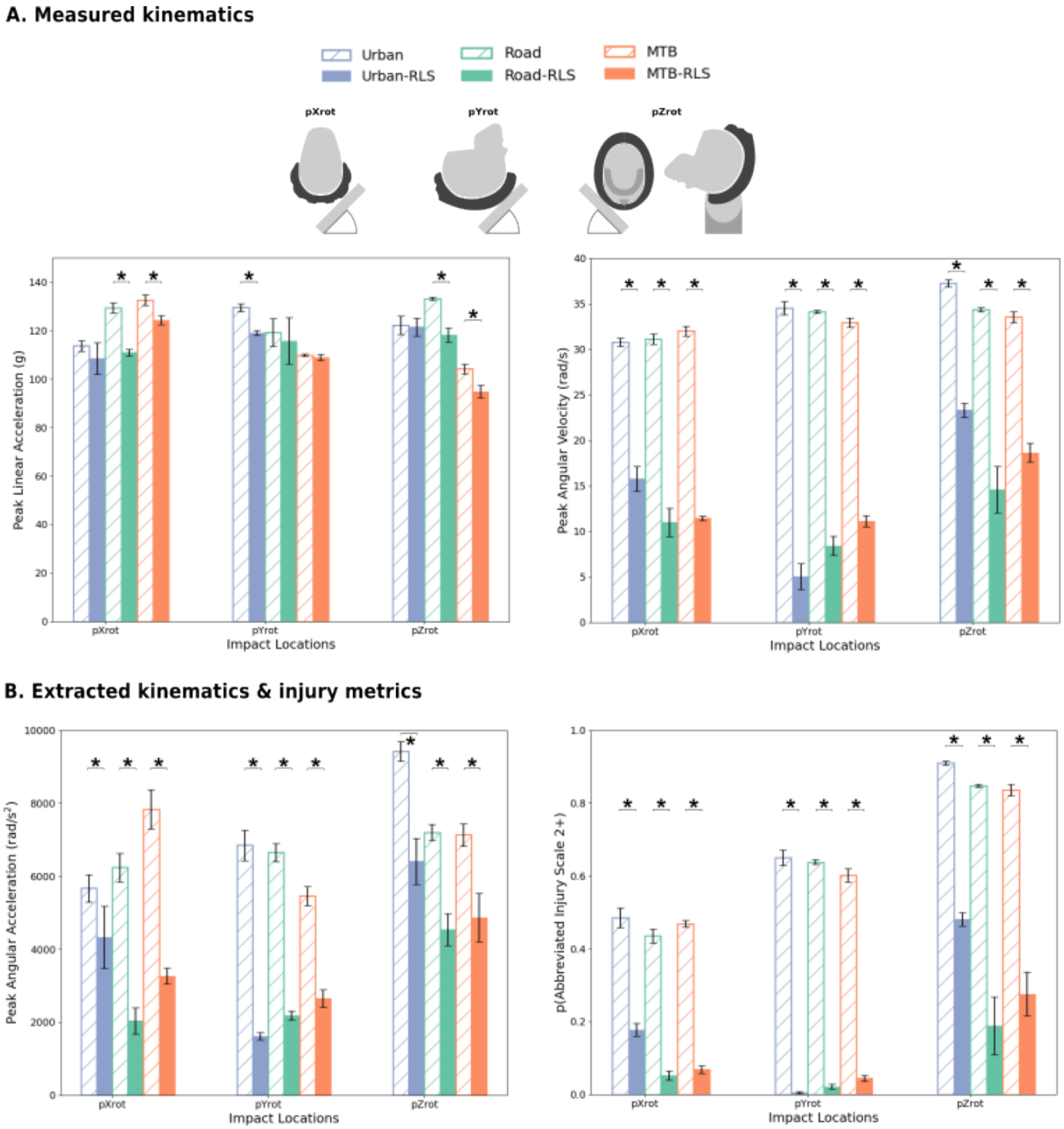

Fig. 4 Data for conventional (hatched) and RLS-equipped helmets (solid) by impact location and helmet type (indicated by color). Peak kinematics (PLA, PRV) as measured by the sensors are shown in A and calculated peak kinematics and injury metrics (PRA, AIS2+) are shown in B, with * indicating $p < 0.05$.

PAV and 44-56% in PAA) across all helmet types, yielding a corresponding reduction in AIS2+ injury probability to 9–22% (Δ_{RLS} of 64–86%). Reductions in PLA (4.5–9.7%) were also observed, although statistical significance was reached only for the road helmet. Both this observation and the variability seen between impact locations (black circles, triangles, and squares representing pXrot, pYrot, and pZrot, respectively, Figure 3) highlight the need for further investigation to better understand the potential effects of helmet geometry and RLS integration.

Table 2 Kinematic and injury metric data for all helmet types per location. When not specified, the differences between control and RLS-equipped helmets were statistically significant with a Mann-Whitney U test statistic of $U = 16.0$, $p = 0.029$.

	Urban					
	pXrot		pYrot		pZrot	
Metric	Control	RLS	Control	RLS	Control	RLS
PLA (g)	113.7±2.1	108.5±6.6	129.5±1.5	119.0±1.1	122.2±3.7	121.5±3.6
	$U = 12.0$, $p = 0.343$		**U = 16.0, p=0.029**		$U = 9.0$, $p = 0.886$	
PAV (rad/s)	30.8±0.5	15.8±1.4	34.5±0.8	5.1±1.4	37.3±0.4	23.3±0.8
PAA (krad/s^2)	5.67±0.37	4.33±0.85	6.85±0.42	1.61±0.10	9.43±0.27	6.41±0.64
BrIC	0.52±0.01	0.34±0.01	0.61±0.01	0.09±0.02	0.82±0.01	0.52±0.01
p(AIS2+)	0.49±0.03	0.18±0.02	0.65±0.02	0.01±0.00	0.91±0.01	0.48±0.02

	Road					
	pXrot		pYrot		pZrot	
Metric	Control	RLS	Control	RLS	Control	RLS
PLA (g)	129.4±2.0	110.9 ±1.3	119.2±5.7	115.7 ±9.6	133.2±0.7	118.3 ±2.9
	U = 16.0, p=0.029		$U = 10.0$, $p = 0.686$		**U = 16.0, p=0.029**	
PAV (rad/s)	31.1±0.6	11.0 ±1.6	34.1 ±0.2	8.4 ±1.0	34.3±0.2	14.6±2.6
PAA (krad/s^2)	6.24±0.39	2.04±0.37	6.65±0.25	2.18±0.13	7.20±0.22	4.54±0.45
BrIC	0.49±0.01	0.21±0.02	0.61±0.00	0.16±0.02	0.75±0.00	0.34±0.06
p(AIS2+)	0.44±0.02	0.05±0.01	0.64±0.01	0.02±0.01	0.85±0.00	0.19±0.08

	MTB					
	pXrot		pYrot		pZrot	
Metric	Control	RLS	Control	RLS	Control	RLS
PLA (g)	132.6±2.3	124.3±1.9	109.8±0.5	108.9 ±1.3	104.2 ±2.0	94.9±2.7
	U = 16.0, p=0.029		$U = 12.0$, $p = 0.343$		**U = 16.0, p=0.029**	
PAV (rad/s)	32.0±0.5	11.4±0.2	32.9±0.5	11.1±0.6	33.5±0.6	18.6±1.0
PAA (krad/s^2)	7.83±0.54	3.27 ±0.22	5.46±0.26	2.65±0.24	7.13±0.30	4.87±0.67
BrIC	0.51±0.00	0.24±0.01	0.58±0.01	0.20±0.01	0.74±0.01	0.40±0.04
p(AIS2+)	0.47±0.01	0.07±0.01	0.60±0.02	0.04±0.01	0.84±0.01	0.28±0.06

Table 3 Percentage reduction between conventional and RLS-equipped urban helmets, Δ_{RLS} when testing with two different headforms, Hybrid III and EN 17950. A Welch ANOVA was utilised to assess the differences in Δ_{RLS} (data for all metrics was normally distributed but not all was homoscedastic).

	pXrot		pYrot		pZrot	
Metric	Hybrid III	EN 17950	Hybrid III	EN 17950	Hybrid III	EN 17950
Δ_{RLS} in PLA (%)	4.5 ± 6.4	-1.9 ± 7.0	8.1 ± 0.7	-2.4 ± 3.1	0.5 ± 4.6	6.0 ± 1.1
	$F(1, 5.96) = 1.79$, $p = 0.229$		**F(1, 3.29) = 42.97, p < 0.001**		$F(1, 3.33) = 5.39$, $p = 0.094$	
Δ_{RLS} in PAV (%)	48.7 ± 4.4	46.5 ± 1.0	85.4 ± 4.01	80.1 ± 2.8	37.4 ± 2.2	41.7 ± 3.7
	$F(1, 3.31) = 0.91$, $p = 0.404$		$F(1, 5.38) = 4.67$, $p = 0.079$		$F(1, 4.85) = 3.82$, $p = 0.110$	
Δ_{RLS} in PAA (%)	23.8 ± 13.9	32.5 ± 6.4	76.5 ± 0.7	80.2 ± 6.6	32.0 ± 6.9	36.9 ± 6.7
	$F(1, 4.24) = 1.31$, $p = 0.313$		$F(1, 3.07) = 1.30$, $p = 0.335$		$F(1, 5.99) = 1.04$, $p = 0.347$	
Δ_{RLS} in BrIC (%)	35.0 ± 3.3	39.3 ± 1.7	85.4 ± 3.7	78.6 ± 3.0	36.7 ± 1.7	42.7 ± 3.3
	$F(1, 4.40) = 5.17$, $p = 0.079$		**F(1, 5.74) = 8.26, p = 0.029**		**F(1, 4.57) = 10.72, p = 0.025**	
Δ_{RLS} in p(AIS2+) (%)	63.3 ± 4.4	71.4 ± 2.2	99.2 ± 0.5	98.4 ± 0.6	47.1 ± 2.3	64.6 ± 5.2
	F(1, 4.38) = 10.73, p = 0.027		$F(1, 5.93) = 4.99$, $p = 0.067$		**$F(1, 4.14) = 38.27$, $p = 0.003$**	

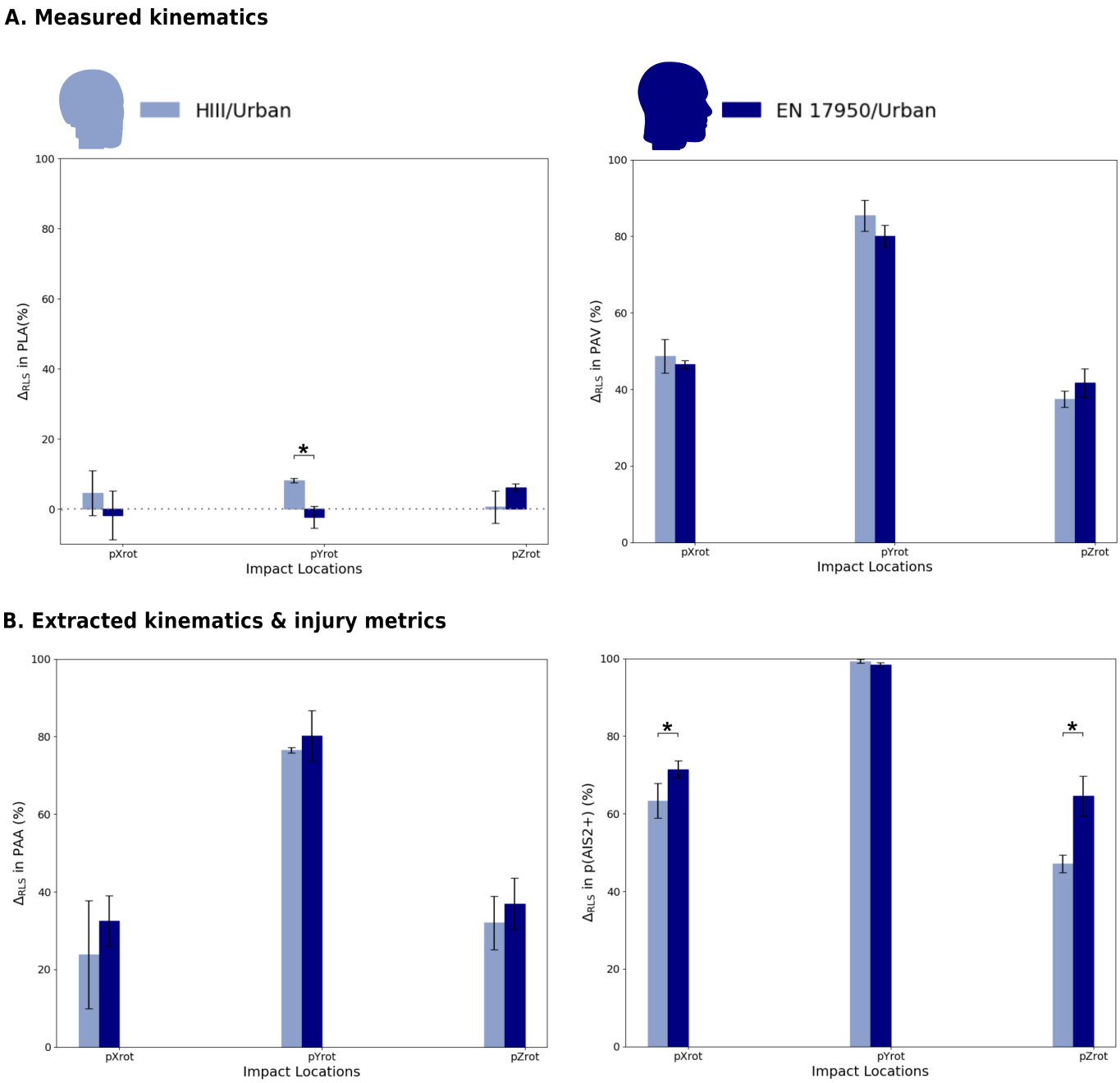

Fig. 5 Percentage reduction by RLS (Δ_{RLS}) for urban helmets, tested with the HIII (light blue) and the EN17950 (navy) headforms.

4.2 Assessment of test results by impact location

Assessing the results at the level of individual impact locations allows for evaluation of repeatability across helmet types and configurations. The coefficient of variation (CV) for kinematic and injury metrics was found to be below 10% for the majority of tests (100%, 78%, 83%, 83%, and 61% of helmets for PLA, PAV, PAA, BrIC, and p(AIS2+), respectively; Figure S1A in Supplementary Information). Instances where CV exceeded 10% were limited to RLS-equipped helmets, with higher variability observed in PAV and p(AIS2+) at the pYrot and pZrot locations. This increase is expected for pYrot, as it is the best-performing location for RLS-equipped helmets that show a substantial reduction in the mean values of rotational kinematics, which in turn elevates CV even when standard deviations remain low (CV = standard deviation/mean). Examining standard deviations provides a more direct comparison with intralaboratory variability reported in literature[25]. In our dataset, standard deviations reached up to 2.6 rad/s for PAV, 850 rad/s^2 for PAA, and 0.08 for p(AIS2+), values consistent with those in the literature, even though our study was conducted at a higher impact speed and impacts at multiple locations (Figure S1B in Supplementary Information). The largest standard deviation for PAV, and thus p(AIS2+), was observed in the pZrot location of the road helmet, likely due to the complex dynamics of this test configuration. Ex-

cluding this case, standard deviations for PAV were within 1.6 rad/s. Overall, the results demonstrate repeatability across impact locations, with the observed variability being consistent with published intralaboratory ranges.

4.3 Trends in performance by impact location

Accident databases and oblique impact testing have shown that impact location plays an important role in brain injury prevalence and severity[28,42–44]. In our dataset, there was a consistent trend in the location-specific rotational kinematics across helmet types but the same trend did not hold across helmet configurations (conventional and RLS-equipped helmets). The effectiveness of RLS-equipped helmets followed a pYrot < pXrot < pZrot trend, whereas conventional helmet effectiveness followed a pXrot < pYrot < pZrot trend (Figure 4). This ranking was consistent across both headforms tested (Figure 5). These findings suggest that geometry alone does not explain the observed differences; system-level effects must also be considered.

Our observations are consistent with prior studies on other rotation-mitigation technologies[27,28]. Bonin et al.[28] hypothesised that the larger improvements at pYrot are linked to the greater radius of curvature of the headform and helmet in the saggital plane, which results in a longer arc length for y-axis compared with x-axis rotations. In the context of RLS, this hypothesis is supported by the orientation of the panels, which are aligned with the helmet's long axis. During a pYrot impact, the panel releases along this axis and follows the larger radius of the headform, remaining in contact with the anvil-headform interface. This configuration allows more spheres to deploy and dissipate energy through rolling. In contrast, during a pXrot impact, the shorter arc length and release along the helmet's short axis provide less coverage of the interface, limiting the number of spheres deployed and the energy dissipated. Integration details can modify this behaviour, as multiple panels may be released depending on the helmet type.

The mechanism differs for pZrot impacts, which involve compound rotations about both the z- and y-axes. The complex kinematics and reduced panel coverage at the impact site likely contribute to the lower effectiveness of RLS in this orientation, though Δ_{RLS} of 37–58% in PAV was still achieved. In addition, rotation around the y-axis shifts the headform's centre of gravity out of balance relative to the helmet, complicating test repeatability and likely contributing to the higher variability observed in PAV at this location (Figure S1B in Supplementary Information). It is also worth noting that in a pZrot impact the rotation around the y-axis brings the centre of gravity of the headform out of balance with respect to the helmet making consistent positioning during testing more challenging. This can potentially explain the high variability observed in some of the data in that orientation.

4.4 Influence of helmet geometry on RLS effectiveness

While the trend in impact location rankings was consistent across helmet types, differences in RLS effectiveness were observed across helmet types suggesting an influence of helmet geometry on RLS performance. In particular, the large, uniform A-surface of the urban helmet, together with its curvature and lack of vents at the pYrot location, provides favourable conditions for RLS deployment. This is reflected in the AIS2+ results (Table 2), which show near-optimal mitigation of mTBI risk at this location. The road and MTB helmets, on the other hand, feature narrower panels at pYrot to accommodate ventilation, reducing RLS coverage and increasing residual kinematics relative to the urban helmet, though risk mitigation remains substantial (Table 2). At the pXrot location, the road and MTB helmets again share similar geometric features—narrow RLS panels combined with vent openings—resulting in comparable rotational performance. These observations demonstrate that RLS effectiveness is shaped not only by impact location but also by helmet geometry. Tuning of the integration of the technology can therefore potentially optimize performance within the design constraints of each helmet type.

4.5 RLS integration effects on linear kinematics

Unlike the reductions in PAV, the ranking of locations in terms of PLA attenuation varied between helmet types. In 3.1, a significant Δ_{RLS} in PLA was detected for road helmets, and in 3.2 and Figure 4, significant reductions were identified across multiple impact locations for all helmet types. This indicates that RLS may influence peak linear kinematics in a location- and geometry-dependent manner. Various hypotheses can be put forward to explain the mechanism behind this. One possibility is that the additional shell functions similarly to the internal injection-molded reinforcements found in low-profile road helmets, stiffening the EPS and limiting splaying under load. The placement of RLS panels may then determine where this reinforcement is most effective. Another hypothesis is that localized forces at the contact points of polycarbonate spheres induce rippling of the underlying EPS surface, producing greater compression in affected regions—akin to coring out small EPS sections at a finer scale. Further experimental work is needed to clarify these mechanisms and to establish whether the observed reductions in PLA represent a consistent and reproducible benefit of RLS integration across helmet types and impact conditions.

4.6 Headform influence

The results in 3.3 indicate that Δ_{RLS} in rotational kinematics (PAV, PAA) was not affected by the headform used. This outcome was expected, as differences in moment of inertia (MoI) and coefficient of friction (CoF) between headforms were hypothesised to influence conventional and RLS-equipped helmets in a similar manner, given that RLS is an thin, outer layer and does not directly interact with the headform surface. Previous studies have shown that MoI and CoF can affect rotational kinematics[28,33,35,45–47], though their relative importance remains debated. Yu et al.[47] further reported a significant interaction between headform and impact location for all injury metrics except brain strain, highlighting the complexity of these factors. Further work is needed to: (a) clarify the relative contributions of MoI and CoF, and (b) determine how CoF may vary over time and orientation, to ensure that the EN 17950 remains biofidelic not only after cleaning but also across repeated testing. This require-

ment is reflected in the EN 17950 protocol, which specifies CoF measurement along both long and short axes[36].

Although headform choice did not significantly affect rotational kinematics, Welch ANOVA tests revealed significant differences in injury metrics (BrIC and AIS2+). These findings emphasize the need for future studies to assess the influence of headform selection on brain injury risk estimation - whether through conventional injury metrics or computational brain models[48,49]. As a preliminary observation, differences in the shape of kinematic traces were noted between headforms. Detailed analysis of full kinematic time series, using tools such as ARCgen[50], may provide further insights into the biomechanical implications of headform selection.

4.7 Limitations and future work

The scope of this study involved certain limitations, which should be acknowledged alongside the opportunities they present for future work. First, all tests were conducted at an impact speed of 6.5 m/s, which is consistent with standard helmet testing but lower than some cycling accident scenarios reported in the literature[51,52]. Additional tests at higher velocities would provide a more complete understanding of RLS performance under severe impact conditions. Second, impact tests were conducted at the pXrot, pYrot, and pZrot locations, representing the most common impact locations found in literature[44]. Testing was not conducted at the nYrot location, which has been also been identified as relevant for cyclist head injuries.

The comparative headform analysis also has constraints. Data were collected only for the urban helmet, selected because it exhibited the smallest average reduction in rotational kinematics across locations and the largest variation in RLS effectiveness between locations. While by testing this helmet we assessed the highest and lowest bound of the RLS effectiveness and whether they change with headform, extending the analysis to include road and MTB helmets would yield a broader evaluation. Moreover, the study assessed the combined influence of headforms and their instrumentation, as different sensor arrays were used. All sensors were calibrated and the same data filtering and analysis protocols were applied, so significant variations due to the sensor arrays are not expected. Another limitation arises from testing across different laboratories. Experiments with the Hybrid III headform were performed at UNISTRA, whereas EN 17950 testing was conducted at HEXR. Although identical protocols were followed, collecting additional EN 17950 data at UNISTRA would have enabled a more direct comparison. This was not feasible due to limited availability of EN 17950 headforms and compatible instrumentation at the time of the study.

Finally, the interaction between headform characteristics and impact location warrants further study. Yu et al.[47] reported significant interactions using an earlier version of the EN 17950, produced by a different manufacturer and tested under earlier validation procedures. Extending our analysis to validate such statistical models with the current, commercially available EN 17950 would be valuable.

5 Conclusions

The present study evaluated the effectiveness of the Release Layer System (RLS), a novel rotation-mitigation technology, compared with conventional EPS helmets of equivalent geometry. Oblique impact testing was conducted across three helmet types, three impact locations, and two headforms (n = 96). RLS-equipped helmets exhibited peak linear accelerations similar to EPS models, with only minor improvements in some cases. In contrast, RLS consistently reduced peak angular velocity, with average reductions of 57–66% across helmet types and locations, corresponding to a 68–86% decrease in the risk of AIS2+ injury. The magnitude of this reduction varied by impact location, with the largest improvements observed in pYrot. Comparative testing with the Hybrid III and the new EN 17950 headforms showed no systematic differences in percentage reductions of angular metrics, though some location-specific differences in injury risk were noted. These findings highlight the potential of RLS technology to substantially reduce rotational injury risk, while also underscoring the need for further work to interpret headform-specific outcomes.

Competing interests

This work was funded by HEXR Ltd. All authors are employees of HEXR Ltd or Dropmatics Ltd, which may benefit from the findings.

Acknowledgements

The authors would like to acknowledge Nicolas Bourdet, Caroline Deck and Rémy Willinger of the iCUBE laboratory of the University of Strasbourg (UNISTRA) for the collection of the oblique impact testing data and the discussion of the results. The authors would also like to thank the whole HEXR team for their contribution to the development of the RLS technology, insightful comments and assistance throughout the study, and in particular James Humphries for his assistance with the graphics. Finally, the authors would like to thank Canyon Bicycles for their support in supplying the MTB helmets.

References

1 CW0302: Proportion of adults who cycle, by any purpose, frequency, and local authority, England, November 2015 to November 2023;. Available from: https://www.gov.uk/government/statistical-data-sets/walking-and-cycling-statistics-cw.

2 World Bicycle Day;. Available from: https://www.europarl.europa.eu/RegData/etudes/ATAG/2022/729463/EPRS_ATA(2022)729463_EN.pdf.

3 European Road Safety Observatory: Facts and Figures – Cyclists - 2023;. Available from: https://road-safety.transport.ec.europa.eu/system/files/2023-02/ff_cyclists_20230213.pdf.

4 Olszewski P, Szagała P, Rabczenko D, Zielińska A. Investigating safety of vulnerable road users in selected EU countries. Journal of safety research. 2019;68:49-57.

5 Guo Y, Liu Y, Wang B, Huang P, Xu H, Bai Z. Trajectory planning framework for autonomous vehicles based on collision injury prediction for vulnerable road users. Accident Analysis & Prevention. 2024;203:107610.

6 GIDAS. GIDAS: German In-Depth Accident Study; 2025. Accessed: 2025-05-12. Available from: https://www.gidas.org/start-en.html.

7 Department of Transport. Road Accidents Safety Data; 2025. Accessed: 2025-05-12. Available from: https://www.data.gov.uk/dataset/cb7ae6f0-4be6-4935-9277-47e5ce24a11f/road-accidents-safety-data.

8 Panagiotaki E, Reinmund T, Mouton S, Pitt L, Shanthini AS, Tubby W,

et al. RobotCycle: Assessing Cycling Safety in Urban Environments. In: 2024 IEEE Intelligent Vehicles Symposium (IV); 2024. p. 357-63.

9 Pucher J, Buehler R. Making cycling irresistible: lessons from the Netherlands, Denmark and Germany. Transport reviews. 2008;28(4):495-528.

10 van Goeverden K, Nielsen TS, Harder H, van Nes R. Interventions in Bicycle Infrastructure, Lessons from Dutch and Danish Cases. Transportation Research Procedia. 2015;10:403-12. 18th Euro Working Group on Transportation, EWGT 2015, 14-16 July 2015, Delft, The Netherlands.

11 Gear Change: A Bold Vision for Cycling and Walking;. Available from: https://assets.publishing.service.gov.uk/media/5f1f59458fa8f53d39c0def9/gear-change-a-bold-vision-for-cycling-and-walking.pdf.

12 Thompson DC, Rivara F, Thompson R. Helmets for preventing head and facial injuries in bicyclists. Cochrane Database of Systematic Reviews. 1999;(4).

13 Olivier J, Creighton P. Bicycle injuries and helmet use: a systematic review and meta-analysis. International journal of epidemiology. 2017;46(1):278-92.

14 Høye A. Bicycle helmets – To wear or not to wear? A meta-analyses of the effects of bicycle helmets on injuries. Accident Analysis & Prevention. 2018;117:85-97. Available from: https://www.sciencedirect.com/science/article/pii/S0001457518301301.

15 Cripton PA, Dressler DM, Stuart CA, Dennison CR, Richards D. Bicycle helmets are highly effective at preventing head injury during head impact: Head-form accelerations and injury criteria for helmeted and unhelmeted impacts. Accident Analysis & Prevention. 2014;70:1-7. Available from: https://www.sciencedirect.com/science/article/pii/S000145751400061X.

16 McIntosh AS, Lai A, and ES. Bicycle Helmets: Head Impact Dynamics in Helmeted and Unhelmeted Oblique Impact Tests. Traffic Injury Prevention. 2013;14(5):501-8.

17 European Committee for Standardization. EN1078:2012 - Helmets for pedal cyclists and for users of skateboards and roller skates. Brussels, Belgium: European Committee for Standardization; 2012. EN1078.

18 Consumer Product Safety Commission. CFR 16 part 1203 - Safety standard for bicycle helmets final rule. Consumer Product Safety Commission; 2012. 16 CFR part 1203. Accessed: 2025-05-12. Available from: https://www.govinfo.gov/app/details/CFR-2012-title16-vol2/CFR-2012-title16-vol2-part1203.

19 AS/NZS 2063:2020 - Helmets for use on bicycles and wheeled recreational devices; 2020. Accessed: 2025-05-12. Available from: https://store.standards.org.au/product/as-nzs-2063-2020?utm_source=standards.org.au&utm_medium=referral&utm_campaign=standards-catalogue.

20 JIS T 8134:2018 - Protective helmets for bicycle users; 2018. Accessed: 2025-05-12. Available from: https://webdesk.jsa.or.jp/preview/pre_jis_t_08134_000_000_2018_e_ed10_i4.pdf.

21 Holbourn AHS. Mechanics of head injuries. The Lancet. 1943;242:438-41.

22 Depreitere B, Van Lierde C, Maene S, Plets C, Vander Sloten J, Van Audekercke R, et al. Bicycle-related head injury: a study of 86 cases. Accident Analysis & Prevention. 2004;36(4):561-7.

23 Emsley B, Farmer J, Sherratt P, Goodall P, Jackson T, West A. An overview of the test methodology used in current cycling helmet standards and literature. International Journal of Impact Engineering. 2024;188:104928.

24 Hansen K, Dau N, Feist F, Deck C, Willinger R, Madey SM, et al. Angular Impact Mitigation system for bicycle helmets to reduce head acceleration and risk of traumatic brain injury. Accident Analysis & Prevention. 2013;59:109-17.

25 Bliven E, Rouhier A, Tsai S, Willinger R, Bourdet N, Deck C, et al. Evaluation of a Novel Bicycle Helmet Concept in Oblique Impact Testing. Accident Analysis & Prevention. 2019;124:58-65.

26 Bottlang M, Rouhier A, Tsai S, Gregoire J, Madey SM. Impact performance comparison of advanced bicycle helmets with dedicated rotation-damping systems. Annals of biomedical engineering. 2020;48:68-78.

27 Abayazid F, Ding K, Zimmerman K, Stigson H, Ghajari M. A new assessment of bicycle helmets: the brain injury mitigation effects of new technologies in oblique impacts. Annals of biomedical engineering. 2021;49(10):2716-33.

28 Bonin SJ, DeMarco AL, Siegmund GP. The effect of MIPS, headform condition, and impact orientation on headform kinematics across a range of impact speeds during oblique bicycle helmet impacts. Annals of biomedical engineering. 2022;50(7):860-70.

29 Baker C, Yu X, Lovell B, Tan R, Patel S, Ghajari M. How well do popular bicycle helmets protect from different types of head injury? Annals of Biomedical Engineering. 2024.

30 Di Landro L, Sala G, Olivieri D. Deformation mechanisms and energy absorption of polystyrene foams for protective helmets. Polymer Testing. 2002;21(2):217-28.

31 Virginia Tech Bicycle Helmet Ratings; 2025. Accessed: 2025-05-19. Available from: https://www.helmet.beam.vt.edu/bicycle-helmet-ratings.html.

32 Group FI. Bicycle Helmets 2023 Tested by Folksam. Folksam Insurance Group; 2023. S41102 23-05. Accessed: 2025-05-19. Available from: https://s7g10.scene7.com/is/content/folksam/S41102_6070pdf.

33 Trotta A, Zouzias D, De Bruyne G, Ní Annaidh A. The importance of the scalp in head impact kinematics. Annals of biomedical engineering. 2018;46:831-40.

34 Zouzias D, Bruyne GD, Annaidh AN, Trotta A, and JI. The effect of the scalp on the effectiveness of bicycle helmets' anti-rotational acceleration technologies. Traffic Injury Prevention. 2021;22(1):51-6.

35 Stark NEP, Clark C, Rowson S. Human Head and Helmet Interface Friction Coefficients with Biological Sex and Hair Property Comparisons. Annals of Biomedical Engineering. 2024;52(10):2717-25.

36 European Committee for Standardization. EN 17950: Protective helmets — Test methods — Shock absorption including measuring rotational kinematics. Brussels, Belgium: European Committee for Standardization; 2024. EN 17950.

37 Hiper Helmet Ratings;. Available from: https://www.hiperhelmets.org/.

38 Willinger R, Deck C, Halldin P, Otte D. Towards advanced bicycle helmet test methods. In: International Cycling Safety Conference; 2014. p. 18-9.

39 International Organization for Standardization. ISO 6487:2015, Road vehicles — Measurement techniques in impact tests — Instrumentation. Geneva, Switzerland: International Organization for Standardization; 2015. ISO6487.

40 Takhounts EG, Craig MJ, Moorhouse KJ. Development of brain injury criteria (BrIC). Stapp Car Crash J. 2013;57:243-66.

41 Association for the Advancement of Automotive Medicine. The Abbreviated Injury Scale 2005, Update 2008. Des Plaines, IL: Association for the Advancement of Automotive Medicine; 2008.

42 Meng S, Gidion F. Bicyclist Head Impact Locations Based on the German In-Depth Accident Study. 2022.

43 Harlos AR, Rowson S. The range of bicycle helmet performance at real world impact locations. Proceedings of the Institution of Mechanical Engineers, Part P: Journal of Sports Engineering and Technology. 2023;237(4):233-9.

44 Baker CE, Yu X, Patel S, Ghajari M. A review of cyclist head injury, impact characteristics and the implications for helmet assessment methods. Annals of biomedical engineering. 2023;51(5):875-904.

45 Cobb BR, Zadnik AM, Rowson S. Comparative analysis of helmeted impact response of Hybrid III and National Operating Committee on Standards for Athletic Equipment headforms. Proceedings of the Institution of Mechanical Engineers, Part P: Journal of Sports Engineering and Technology. 2016;230(1):50-60.

46 Lindgren N, Halldin P, Fahlstedt M. Influence of Headform on As-

sessments and Ratings of the Protective Performance of Bicycle Helmets. In: Conference Proceedings International Research Council on the Biomechanics of Injury, IRCOBI; 2022. .

47 Yu X, Halldin P, Ghajari M. Oblique impact responses of Hybrid III and a new headform with more biofidelic coefficient of friction and moments of inertia. Frontiers in Bioengineering and Biotechnology. 2022;Volume 10 - 2022. Available from: https://www.frontiersin.org/journals/bioengineering-and-biotechnology/articles/10.3389/fbioe.2022.860435.

48 Zhou Z, Fahlstedt M, Li X, Kleiven S. Computational helmet ranking outcome is affected by the choice of injury metrics. In: 2024 International Research Council on the Biomechanics of Injury, IRCOBI 2024, Stockholm, Sweden, Sep 11 2024-Sep 13 2024. International Research Council on the Biomechanics of Injury; 2024. p. 486-7.

49 Fahlstedt M, Abayazid F, Panzer MB, Trotta A, Zhao W, Ghajari M, et al. Ranking and rating bicycle helmet safety performance in oblique impacts using eight different brain injury models. Annals of biomedical engineering. 2021;49:1097-109.

50 Hartlen DC, Cronin DS. Arc-length re-parametrization and signal registration to determine a characteristic average and statistical response corridors of biomechanical data. Frontiers in Bioengineering and Biotechnology. 2022;10:843148.

51 Bourdet N, Deck C, Carreira RP, Willinger R. Head impact conditions in the case of cyclist falls. Proceedings of the Institution of Mechanical Engineers, Part P: Journal of sports engineering and technology. 2012;226(3-4):282-9.

52 Bourdet N, Deck C, Serre T, Perrin C, Llari M, Willinger R. In-depth real-world bicycle accident reconstructions. International journal of crashworthiness. 2014;19(3):222-32.